SPECTRAL WAVE DISSIPATION BASED ON OBSERVATIONS: A GLOBAL VALIDATION

Fabrice Ardhuin*, Fabrice Collard**, Bertrand Chapron***, Pierre Queffeulou***, Jean-François Filipot*, Mathieu Hamon****

* Service Hydrographique et Océanographique de la Marine, 29609 Brest, France
** BOOST-Technologies, 29280 Plouzané, France
*** Laboratoire d'Océanographie Spatiale, Ifremer, 29280 Plouzané, France
**** Laboratoire de Physique des Océans, Université de Bretagne Occidentale, 29238 Brest, France

Abstract:

Existing parameterizations of wave dissipation used in spectral wave models have provided excellent results in most of the world ocean, but lead to significant and persisting errors. Here a new parameterization is proposed that simply combines the observed swell dissipation and a saturation-based dissipation compatible with observed wave breaking probabilities. This parameterization is adjusted to provide an accurate hindcast of the global wave field as observed by in situ buoys, and a preliminary validation is presented. The resulting global model is shown to outperform all existing operational models to date in terms of significant wave height, and peak and mean periods. The model further provides a better rendering of the high frequency part of the wave spectrum, as validated with C-band radar altimeter cross sections, with important applications for remote sensing. Improvement and adjustment of the model is in progress, with a view to further improving high frequency waves and coastal sea states.

I. INTRODUCTION

A. Generalities

For the last 50 years, spectral wave modeling has been largely based on the wave energy balance equation [1], which describes the radiation of the spectral density of the surface elevation variance F distributed over frequencies f and directions θ,

$$\frac{dF}{dt} = S_{atm} + S_{nl} + S_{oc} + S_{bt} \qquad (1)$$

where the Lagrangian derivative is the rate of change of the spectral density when following a wave packet at its group speed in physical and spectral space. The source function on the right hand side is separated into an atmospheric source function $S_{atm}(f,\theta)$, a nonlinear scattering term $S_{nl}(f,\theta)$, an ocean source $S_{oc}(f,\theta)$, and a bottom source $S_{bt}(f,\theta)$. This separation is somewhat arbitrary, but, compared to the usual separation of deep-water evolution in input, non-linear interactions, and dissipation, it has the benefit of identifying where the energy is going to or coming from. S_{atm} gives the flux of energy from the atmospheric non-wave motion to the wave motion, it is the sum of a wave generation term S_{in} and a wind-generation term (often referred to as negative wind input, i.e. a wind output) S_{out}. The nonlinear scattering term S_{nl} represents all processes that lead to an exchange of wave energy between the different spectral components. In deep and intermediate water depth, this is dominated by cubic interactions between quadruplets of wave trains [2,3], while quadratic nonlinearities play an important role in shallow water [4]. The ocean source S_{oc} may accommodate wave-current interactions and interactions of surface and internal waves, but here it is restricted to wave breaking and wave-turbulence interactions, and the dissipation of wave energy in the ocean bottom boundary layer. Finally, interactions with the bottom will not be considered here, and are discussed elsewhere [5,6]. The basic principle underlying eq. (1) is that waves essentially propagate as a superposition of linear wave groups with a weak-in-the-mean evolution due the processes listed above.

Recent reviews have questioned the possibility of further improving numerical wave models without changing these basic principles [7]. Although this may be true in the long term, we demonstrate here that it is still possible to improve model results significantly by including more physical constraints in the source term parameterizations. The main advance proposed in the present paper is the adjustment of a shape-free dissipation function based on today's knowledge on the breaking of random waves [8,9] and the dissipation of swells over long distances [10].

B. Deficiencies of the WAM-Cycle 4 family of parameterizations

Models that use the dissipation parameterizations of the form proposed by Komen et al. [11] have been refined over the last 25 years [12] with the introduction of new features [13]. In spite of their relative success for the estimation of the significant wave height H_s and peak period T_p, the original

fixed-shape dissipation functions have terrible built-in defects, like the spurious effect of swell on wind sea growth, with stronger growth modeled with higher swells, as shown on figure 1, and discussed in [14].

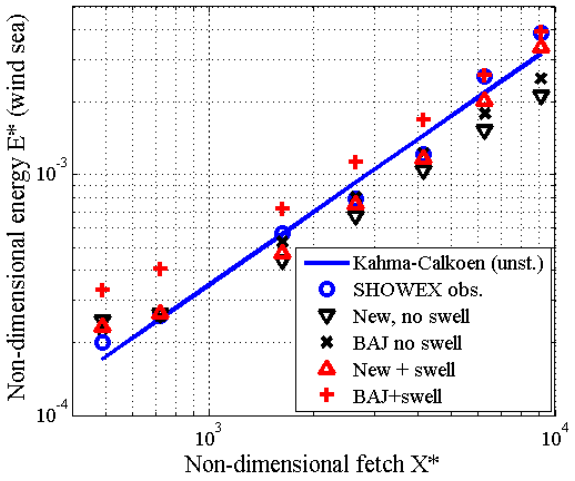

Figure 1. Fetch-limited growth during the 9.5 m/s wind case of SHOWEX, discussed in [14]. The BAJ parameterization [12] is particularly sensitive to swell at short fetch (differences between × and + symbols). The new dissipation term, described below is not sensitive to swell, and allows a better fit to the observations. Differences at large fetch are an artifact of the sea-swell separation.

Associated with that defect also comes a strong reduction of high frequency energy. Both effects are due to the use of a mean steepness for the entire spectrum, defined from a mean wavenumber $\langle k \rangle$, with the peak and low frequency dissipated at a rate proportional to $k / \langle k \rangle$, which generally decreases when swell height increases, and the high frequency dissipated at a rate proportional to $k^2 / \langle k \rangle^2$ which increases with swell height.

The high frequency energy level depends on the balance of all source terms. Here we use a WAM-Cycle 4 form, as modified by [12], and verify the adequacy of this high frequency dissipation using C-band normalized radar cross sections σ_0 from the JASON satellite altimeter. The values of σ_0 have been reduced by 1.2 dB to fit other C-band observations [15]. The observed filtered mean square slope is given by [16], $mss_C = 0.64/\sigma_0$.

The C-band mss is obtained from the model-integrated mss in the band 0.03 to 0.72 Hz by adding a constant of 0.015, which corrects the bias at the peak of the distribution and is meant to represent the unresolved high frequency waves that are present in the altimeter measurements but not in the model calculation. In the new model parameterization, described below, this correction is only 0.011. The model uses a maximum effective frequency $f_{max} = \max\{0.72 \text{ Hz}, 2.5\ f_m, 2.5\ f_{mwg}, 4\ f_{PM}\}$, where f_m is the mean frequency corresponding to the mean period $T_{m0,-1}$, f_{mwg} is the same parameter with a spectral integral restricted to the part of the spectrum where the wind-wave interaction term S_{atm} is positive, and f_{PM} is the Pierson-Moskowitz peak frequency for the local wind speed. For $f > f_{max}$, the spectrum is extrapolated to 0.72 Hz using a f^{-5} tail.

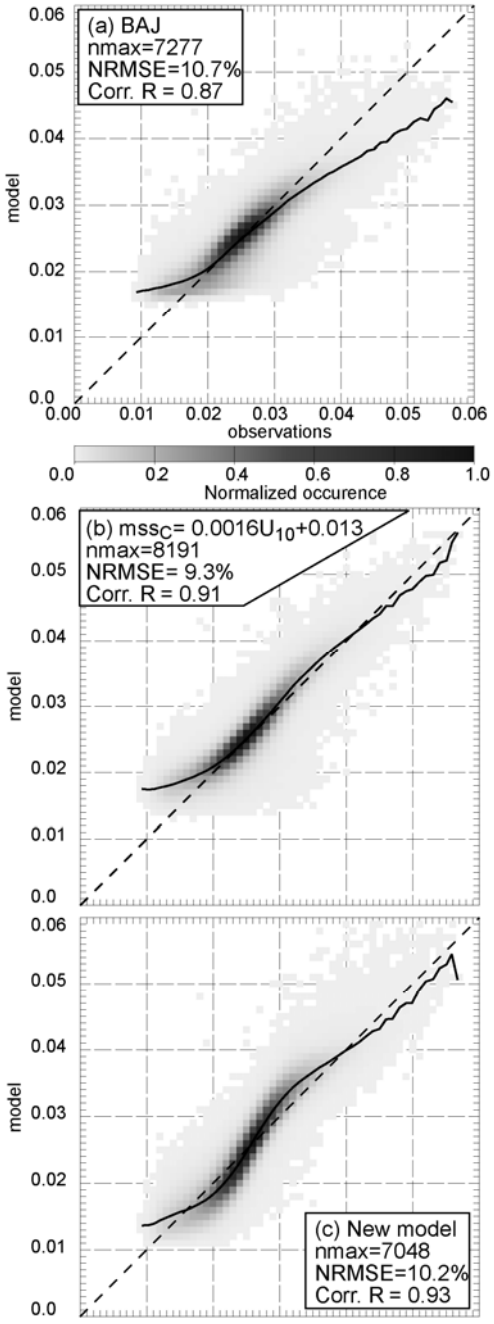

Figure 2. Modelled versus observed filtered mean square slopes for January to June 2007 over the globe. Observations are obtained from JASON's C-band altimeter. (a) Model with BAJ parameterization, (b) simple empirical model based on the ECMWF wind speed: $mss_C = 0.013 + 0.0016\ U_{10}$, (c) new model. Gray scales show the normalized number of occurrences in each 0.001 by 0.001 bin.

Model and satellite data were averaged in space and time along the satellite track, over 8 seconds segments, taking 1 Hz data every two points.

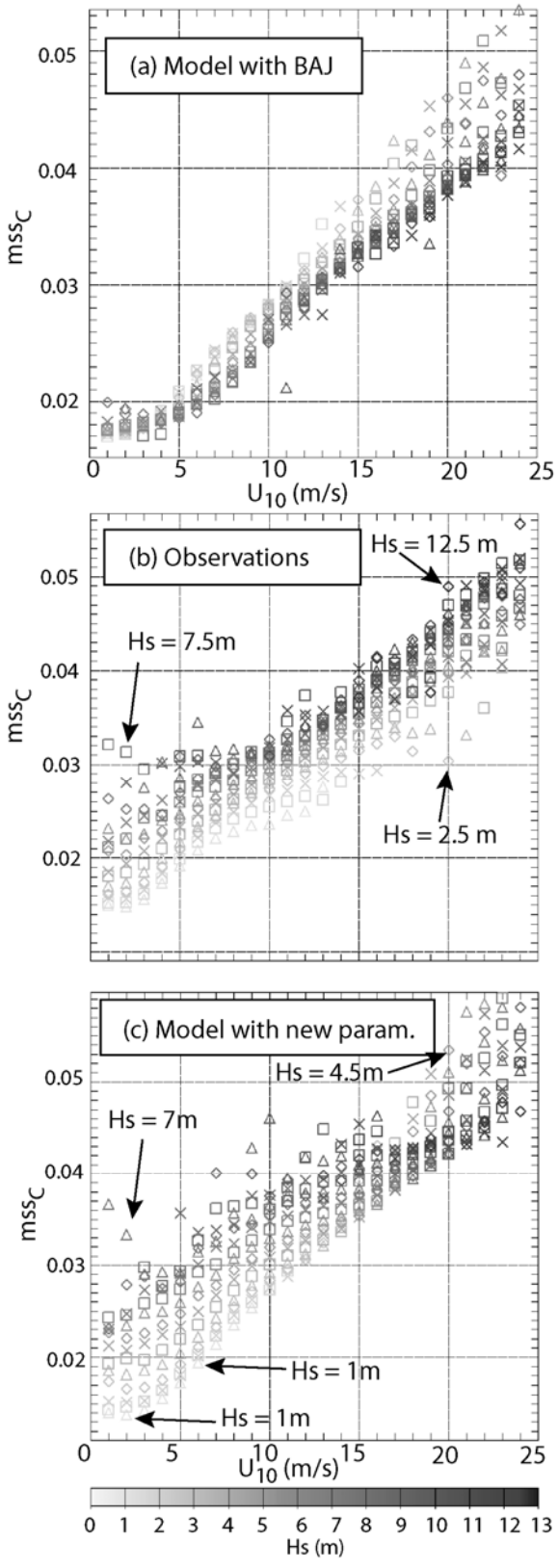

Figure 3. Mean value of mss_C binned as a function of U_{10} (x-axis) and H_s (gray scales). H_s classes are 0.5m wide and range from from 1 to 12.5m. U_{10} classes are 1 m/s wide. (a) Model with BAJ parameterization, (b) observations, (c) new model. For better readability, the symbols cycle through Δ (1, 3, 5 m …), □ (1.5, 3.5, 5.5m), × (2, 4, 6 m, …) and ◊ (2.5, 4.5, 6.6 m >...).

The BAJ parameterization leads to poor surface slope statistics (figure 2), making it ill-suited for remote sensing applications. Although the method for derive the C-band mss could be improved [17], the model sensitivity to swells results in a Pearson's correlation coefficient between the altimeter data and the model-derived mss that, at 0.87, is lower than the correlation of the mss_C with the wind used to drive the model (0.91, figure 2b).

Indeed, mss_C is essentially a function of the wind speed U_{10} and the wave height, a surrogate variable for both swell and wave age [17]. The model behavior appears more clearly when binning the data as a function of these two variables (figure 3). The BAJ parameterization for U_{10} > 3 m/s gives higher mss_C for lower wave heights, contrary to the observations. This defect is also shared by the new parameterization for U_{10} > 17 m/s, which is likely due to the abusive use of a f^{-5} for $f > f_{\max}$, which is as low as 0.3 Hz for these large wind speeds. For the low wind speeds the paradoxical behaviour of mss_C is another artifact of the mean steepness through the $k^2/\langle k \rangle^2$ dissipation term. In the new parameterization, defined, below there is no influence of one frequency on another, which is more realistic, but apparently exaggerated. Indeed, the spread of mss_C at $3<U_{10}<10$ m/s is larger in the new parameterization than in the observations. This confirms the finding of [17], that the mean square slope due to the short waves is weakly reduced in the presence of swell.

Another widely used alternative parameterization has been proposed by Tolman and Chalikov [18]. Their formulation contains important features that we borrow in the present formulation. Namely, the dissipation is essentially a function of the local spectral density in the frequency spectrum, and a negative wind input plays a major role in the swell evolution. However, the magnitude of the source terms appear too weak, as the parameterization yields important biases in wave growth and wave directions at short fetch [14]. Finally, the separation of the two types of dissipation at low and high frequency could have corresponded to the separation between wave breaking (high frequency) and other processes (low frequency). However, it is now well established that this separation cannot be set at twice the peak frequency, since even dominant wave break in young seas. A complete redesign of the source terms is thus necessary.

II. A SPECTRAL DISSIPATION SOURCE FUNCTION

A. Wave breaking

Observations show that no dominant waves break when a non-dimensional form of the local spectral level exceeds a threshold [8] which is larger for broader directional spectra [19]. Other observations show that waves break when the orbital velocity at the crest exceeds a factor 0.7 to 1 times the phase velocity [20,21]. We further propose that the statistics of breaking waves are controlled by linear dispersion and superposition of wave trains to form wave groups. The orbital velocity criterion leads us to define a direction-weighted saturation spectrum

$$B(f,\theta) = 2\pi \int_{\theta-\Delta}^{\theta+\Delta} k^3 \cos^p \theta' F(f,\theta')/C_g d\theta' \qquad (2)$$

which, with p=2, is related to the maximum orbital velocity in direction θ for waves with frequencies close to f, normalized by the phase velocity. A detailed justification requires the definition of individual wave statistics from spectral parameters [22,23], and is beyond the scope of the present note. For any frequency wave breaking is expected to occur first in the main wave direction θ_0 for which

$$B(f,\theta_0) = B_0(f) = \max\{B(f,\theta), \theta \in [0,2\pi[\} \quad (3)$$

Thus, in deep water, taking a fixed threshold B_r to characterize the lowest detectable probability of breaking is generally consistent with all observations. In shallow water a proper extension of (2) can be given to represent the different wave kinematics. Following [8] and [19] we assume that the breaking probability for any given wave scale is proportional to B-Br. We now define the breaking severity as the dissipation rate per each breaking wave normalized by the breaking wave energy. We further hypothesize, which is quite questionable, that the severity is also proportional to B-Br. Because the energy of the breaking waves is a convolution of the breaking rate by the spectral content of the waves, we approximate the spectral dissipation rate as the triple product of the spectral density, breaking probability, and breaking severity.

$$S_{ds}(f,\theta) = \sigma C_{ds} \left\{ \delta \left[\max\left\{ \frac{B_0}{B_r} - 1,0 \right\} \right]^2 + (1-\delta) \left[\max\left\{ \frac{B}{B_r} - 1,0 \right\} \right]^2 \right\} F(f,\theta) \qquad (4)$$

The use of the two terms, the first isotropic and the second non-isotropic, is an *ad hoc* way of deconvoluting the breaking probabilities back to the spectrum, and also possibly of accounting for cumulative effects [9]. Indeed waves break because of their intrinsic kinematics, but also because they are swept away by larger breaking waves, an effect which is neglected here. According to [9] when p=0 and Δ=180°, the threshold level is B_r=0.0012. With p=2 we have adjusted the threshold value to B_r=0.0008, which is gives the same threshold for a 35° directional spread or $\cos^{1.5}$ direction distribution.

The source function (4) was implemented in version 3.14a of the WAVEWATCH code framework [24]. The dissipation constant C_{ds} was adjusted using the DIA parameterization for nonlinear wave-wave interactions [25], and the wind input parameterization used in the ECWAM model [12] in which the maximum growth rate β_{max} was increased from 1.25 to 1.55 to compensate for a reduction of the wave age correction factor z_α from 0.011 to 0.006, which reduces the growth of waves with phase speeds close to that of the wind. We note that β_{max}=1.25, used in the BAJ runs presented here, is already larger than 1.2 used at ECMWF). The growth curves for H_s are well reproduced (Figure 1) together with the frequency spectra and the directional distribution of wave energy (Figure 4), provided that a non-isotropic dissipation is used.

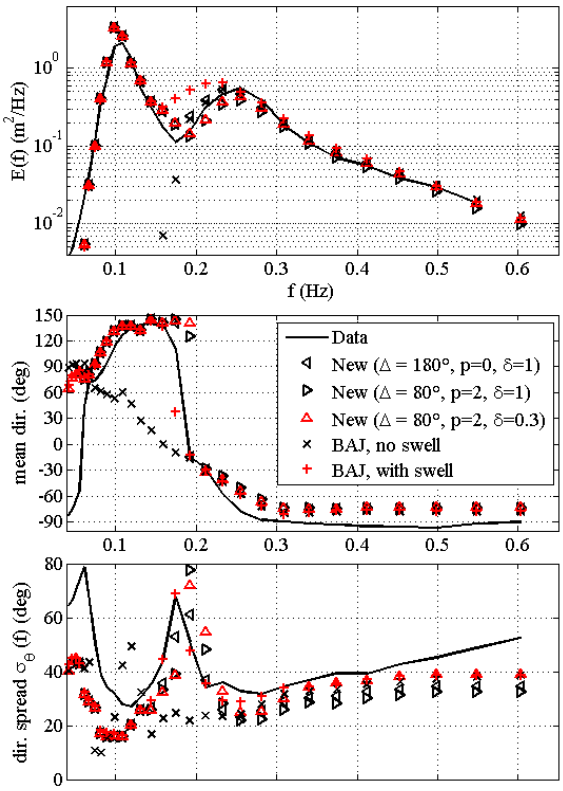

Figure 4. Fig. 3. Model-data comparison at buoys X3, at a fetch of 39 km, during the SHOWEX event discussed in [14], with a wind speed of 9.5 m/s. (a) Frequency spectra, (b) mean directions, (c) directional spreads. Model results are obtained with the BAJ [12] parameterization with our without the incoming swell, and the new dissipation function with isotropic (δ=1) ot non-isotropic dissipations.

Further tests have shown that, for high winds (> 15 m/s) the dissipation is generally insufficient at high frequency. This is already visible in figure 3.c. At present, this problem is corrected (too strongly) by the use of a diagnostic f^{-5} tail beyond a maximum frequency f_{max} defined from the mean frequency of the wind-generated part of the spectrum [12]. For example, a typical wind sea in the open ocean with a wind of 15 m/s gives f_{max} = 0.34 Hz. It is expected that a proper parameterization of the cumulative effect [9] will properly correct for this error.

B. Swell dissipation

A very important part of the parameterization, at least when considering oceanic scales, is the dissipation of swells. Historically, swell has been a process which is now regarded as negligible [26]. Recent theories have instead focused on air-sea interactions, and, in particular the correlation of pressures and surface slopes over swells [27]. Progress in this area was hampered by the lack of

reliable estimate of the swell dissipation. This has now changed with the analysis of swell propagation using synthetic aperture radar (SAR) [10]. The main finding of this investigation is that swell decay is non-linear, with a relative stronger decay of steeper swells, and there are indications that there is a threshold steepness below which dissipation is negligible. Taken together, these facts support that swell dissipation is dominated by friction in the air-side boundary layer. Because this process yields a net momentum flux to the atmosphere, which generates wind [28], the corresponding source term will be called here "wind output". The oscillatory boundary layer is expected to be laminar or turbulent depending on the Reynolds number Re=2uorbHs /va, where va is the air viscosity, and the significant orbital velocity amplitude is

$$u_{orb} = 2\int_0^{2\pi}\int \sigma^2 F(f,\theta)\,d\theta\,df \qquad (5)$$

For Re < Rec, the swell dissipation source term for swells is given by the viscous theory [29],

$$S_{out}(f,\theta) = -s_5 \frac{2\rho_a}{\rho_w} k\sqrt{2\sigma\nu_a}, \qquad (6)$$

where s_5 is a tuning coefficient: s_5=1 for clean water surfaces. Here we shall take s_5=1.2. For Re > Re_c, the turbulent dissipation can be parameterized as

$$S_{out}(f,\theta) = -\frac{\rho_a}{\rho_w} 16 f_e \frac{\sigma^2 u_{orb}}{g} F(f,\theta), \qquad (7)$$

Consistent with fixed bottom boundary layers, it was observed that $Re_c \approx 10^5$, the value used here.

Using a wave model to estimate the full orbital velocity (i.e. including the wind sea), the dissipation factor f_e may be estimated form the SAR observations (figure 5).

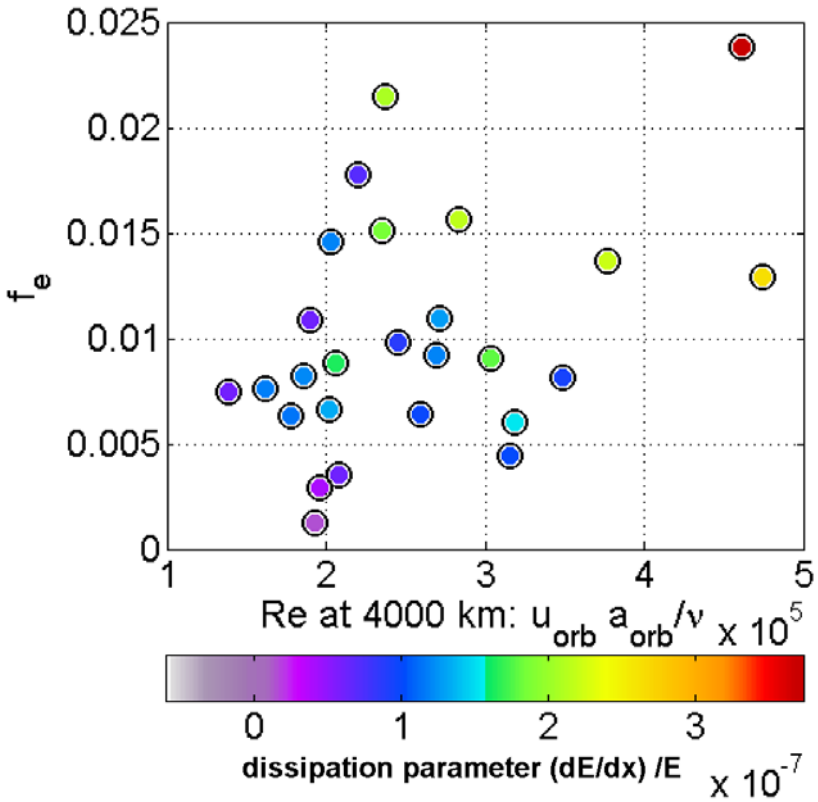

Figure 5. Dissipation factor f_e as a function of the Reynolds number for swells 4000 km away from their generating storm. The colors show the corresponding spatial decay parameter, inferred by fitting theoretical dissipation curves to the observed variation in swell wave height. Each dot correspond to one swell system from one storm, followed from 4000 to 8000 or more kilometers away from the storm center [10].

Most of the values of f_e fall in the range 0.005 to 0.01, slightly higher than smooth boundary layer observations [30] which, for similar Reynolds numbers, are in the range 0.004 to 0.007. The larger values of f_e are probably overestimated due to a general underestimation of H_s, and thus u_{orb}, in the biggest storms. It was found that the model tended to underestimate large swells and overestimate small swells. This defect is likely due, in part, to errors in the generation or non-linear evolution of these

swells. However, it was chosen to adjust f_e as a function of the wind speed and direction,

$$f_e = 0.7\, f_{e,GM} + \left[0.015 - 0.018\cos\left(\theta - \theta_u\right)\right]\frac{u_*}{u_{orb}}, \quad (8)$$

where $f_{e,GM}$ is the friction factor given by [31] for rough oscillatory boundary layers without a mean flow, using a roughness length adjusted to 0.04 times the roughness for the wind. Eq. (8) gives a stronger dissipation for swells opposed to winds.

III. MODEL PERFORMANCE

All model runs discussed here are performed using version 3.14a of WAVEWATCH [24] kindly provided by H. Tolman for development and beta testing. The model configuration used is global with 0.5° regular resolution in latitude and longitude. The spectral grid uses 32 frequencies from 0.0373 to 0.716 Hz, and 24 directions. The model is forced with analyzed wind and sea ice concentration every 6 hours with the same spatial resolution, provided by the European Center for Medium Range Weather Forecasting (ECMWF). These fields are interpolated in time, preserving the square of the wind modulus. Further, subgrid islands are treated using a masking coefficients based on a coastline database [32].

Besides the sensitivity to swells in coastal areas (figure 1, 4), the main motivation for designing a new source term package was the overestimation of swell heights and periods in the Pacific, a feature common to all the parameterizations derived from [11] but absent in [18]. In addition, we also desired a proper variability of the high frequency tail level, for remote sensing applications (figure 2). Here we will focus on parameters that are more widely used for ocean and coastal engineering, namely H_s, the peak frequency f_p or peak period T_p and the mean period $T_{m,02}$.

The global biases against altimeters have been dramatically improved, with the positive values in the East Pacific, and East Indian ocean now almost completely erased (figure 6). In fact, it is likely that swell heights are now slightly underestimated in these areas. From the analysis of swell propagation using SAR data, it appears this is rather due to an underestimation of swell generation in the most severe storms, together with an overestimation of the dissipation of more moderate swells. Work is under way to further adjust the parameterizations in order to correct these errors.

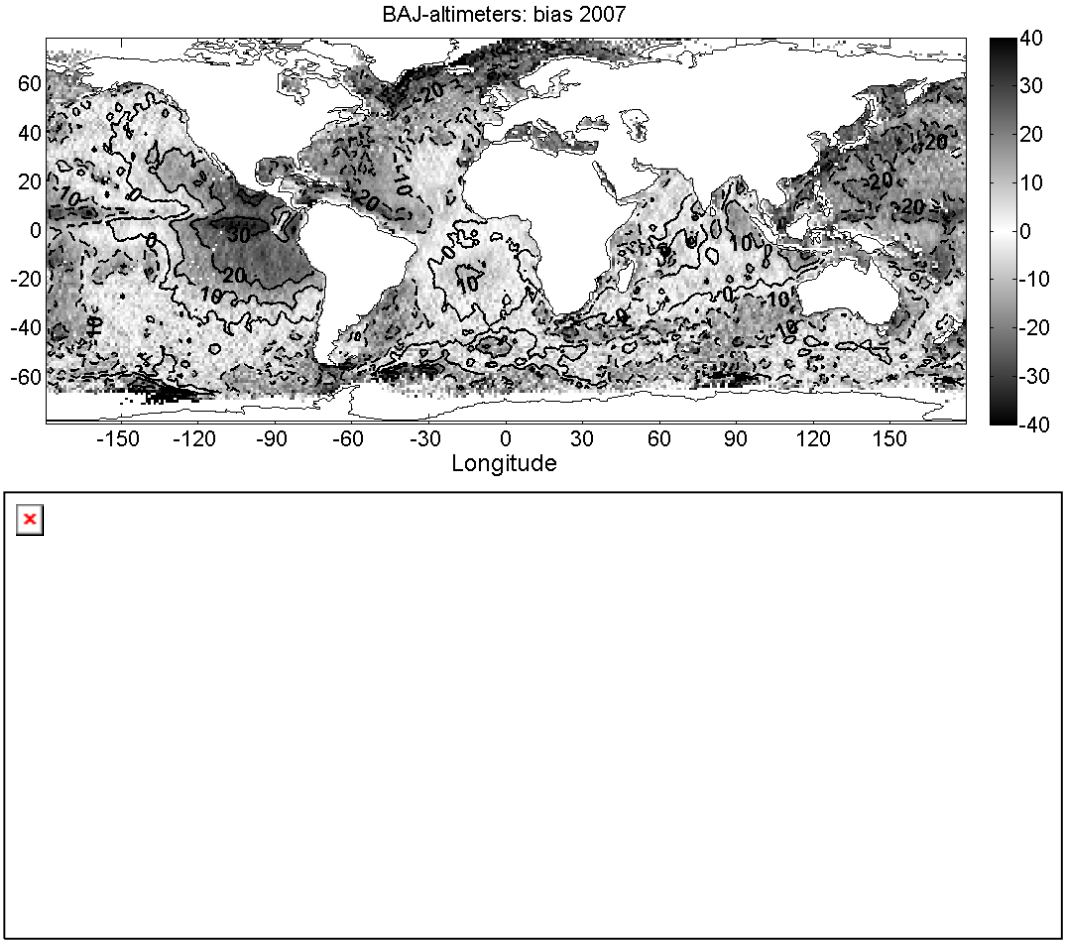

Figure 6. Mean difference in centimeters between modeled and observed wave heights for the year 2007. Observations combine of data from JASON, ENVISAT and GEOSAT-Follow on (GFO) altimeters, with a method described in [33]. Results are provided for (top) the BAJ parameterization, (bottom) the new parameterization described here.

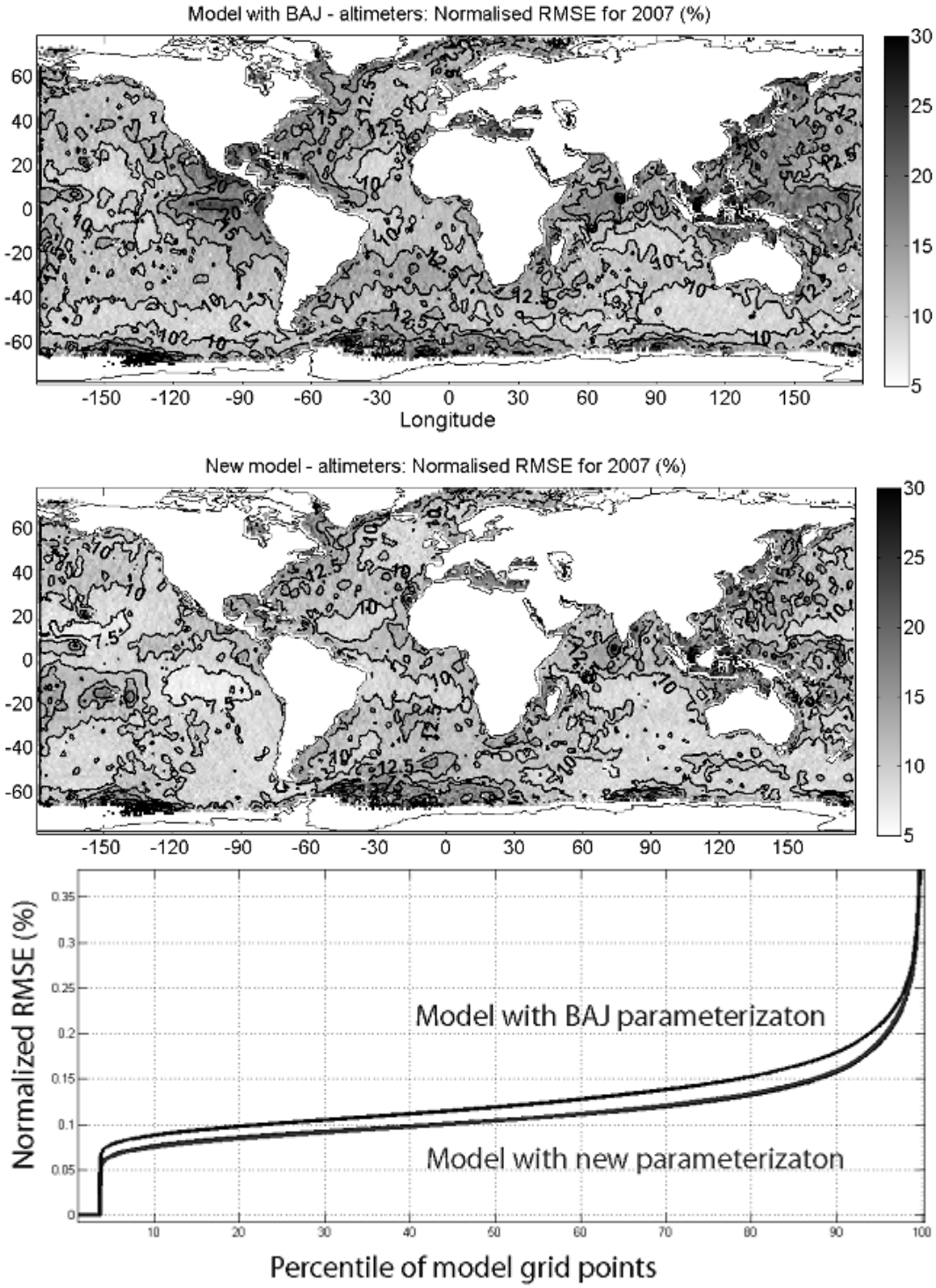

Figure 7. Top two panels: same as figure 6, here showing the Normalized root mean square error (NRMSE) instead of the bias. The additional bottom panel shows the percentile distribution of model grid points with a given normalized errors (in percent): the top curve is the model with BAJ, and the bottom curve corresponds to the new model.

Interestingly, the East-West gradient in the wave height bias found with the BAJ parameterization is greatly reduced. This was already the case with the parameterization of Tolman and Chalikov [18], as revealed in [32]. We believe that this is because there is generally less swell on the Western side of ocean basins. With less swell the BAJ parameterization gives a lower windsea growth, and leads to the previously found bias.

The root mean square errors (RMSE) are also greatly reduced. When normalized by the RMS observation at each grid point, the resulting normalized error (NRMSE) is generally reduced by 1.7 percentage points, from 13.1% to 11.4% when averaged over the globe (table 1), with a median error now just over 10% (figure 6). The fraction of model grid points where the NRMSE on H_s is less than 10%, has expanded from 19% with BAJ to 42% with the new parameterization. The median error

with BAJ is reduced from 12% to 10.5%. There is even 11% of the world ocean with errors on H_s under 8%, while only 2% had such a low error with BAJ. Random errors are reduced in the trade winds and in the western boundaries of ocean basins (see figure 6: East of Japan, U.S. East coast, Northern Indian ocean, East coast of Australia).

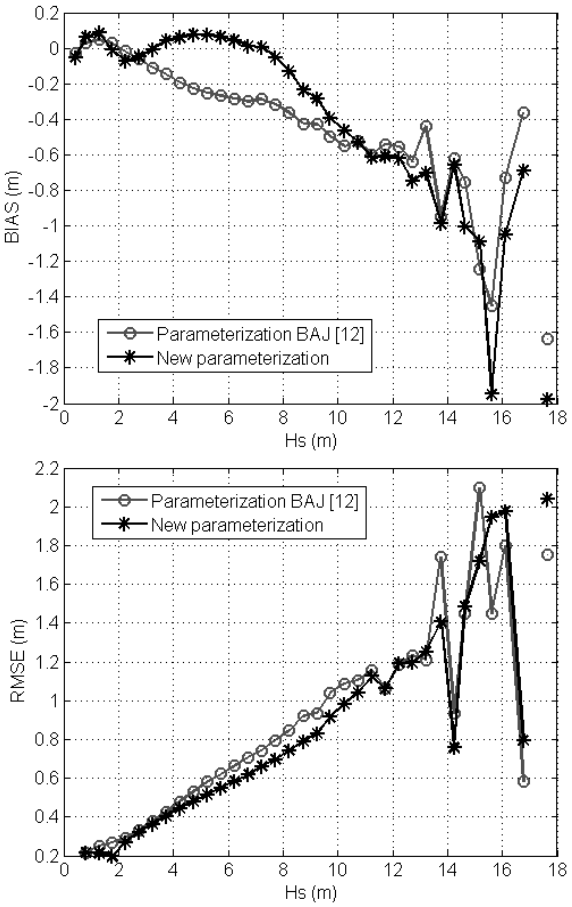

Figure 8. Bias (top) and root mean square error (bottom) in meters for several model parameterizations against all three altimeters for the year 2007, as a function of wave height.

Model errors were also analyzed as a function of H_s in order to investigate a possible underestimation of storm peaks [35]. Although the model has virtually no bias for H_s up to 8 m, there is a general underestimation above 10 m, as with all the other parameterization investigated here. This bias reaches 7% at 14 m. Above 14 m, not enough satellite data are available in one single year to provide reliable statistics (figure 7). The present parameterization gives the lowest RMSE for wave heights up to 14 m.

The model results were also compared against all available *in situ* data for the entire year 2007 [10]. The buoys considered here are those with WMO numbers 41002, 41010, 42001, 42002, 42003, 44004, 44008, 44011, 44137, 44138, 44139, 4414 (U.S. and Canadian East coasts and Gulf of Mexico), 46001, 46004, 46035, 46066, 46184, 46002, 46005, 46036, 46059 (U.S. and Canadian west coasts), 51001, 51002, 51003, 51004 (Hawaii), 62029, 62081, 62163, 64045 (North East Atlantic). The values for T_p correspond to all the American buoys, while the values for T_{m02} correspond only to the 4 European buoys.

TABLE I.
NORMALIZED RMSE FOR VARIOUS MODEL RUNS AGAINST ALTIMETER AND IN SITU DATA, FOR YEAR 2007. THE ECMWF RUN IS ECMWF'S OPERATIONAL ANALYSIS, GIVEN HERE FOR REFERENCE.

Model run	New	BAJ	ECMWF
Altimeters H_s	11.4%	13.1%	
Altimeters mss_C	10.2%	10.7%	
Buoys H_s	12.4%	13.6%	11.0%
Buoys T_p	19.8%	24.1%	16.9%
Buoys T_{m02}	6.8%	7.6%	8.5%

IV. SUMMARY AND DISCUSSION

Parameterizations for wind wave generation and evolution have been constantly refined over the last few decades. The dissipation terms based on an overall mean steepness for the entire spectrum [11], culminated in the parameterization (BAJ) used at present at ECMWF [12]. That parameterization, until recently, provided the best available analysis and forecasts of sea states for most applications. Here we present a new set of parameterizations that combine a wave breaking parameterization compatible with the threshold behavior of breaking statistics [8,9], and a nonlinear swell dissipation consistent with observed swell decays [10]. Although many details of this parameterization are still to be refined, these two important features remove the spurious swell sensitivity in the BAJ parameterization, leading to a better estimate of common wave parameters at global scales, as summarized in table 1. Here we presented an extensive validation, using in situ and remote sensing, data, including, for the first time, altimeter radar cross sections. The model has been validated by global 4 year hindcast, avaialable via ftp at ftp://ftp.ifremer.fr/ifremer/cersat/products/gridded/wavewatch3/, and is routinely used for forecasting since May 10, 2008, in a version similar to the one described here, and since July 17 in this exact form. In enclosed areas, where little altimeter data can be used to correct the model by assimilation, the model presented here actually provides the best operation analyses and forecasts so far. This will become clearer in the statistics for the coming months presented in the JCOMM model verification page http://www.jcomm-services.org/Wave-Forecast-Verification-Project.html/.

The present parameterization gives the best result so far for in terms of biases and random errors, but it still underestimates high frequency dissipation, which is now largely hidden by the use of a diagnostic tail. There is also an underestimation of the largest wave heights which may be due to many factors: quality of the wind forcing, lack of proper parameterizations for sea states with many breaking waves…. However, the mean square slopes derived from C-band

altimeter data suggest that the parametric tail is likely responsible for an important part of this underestimation. Further work will focus on correcting these effects, and validating the model at coastal scales. For this, the directional distribution of the wave energy is of critical importance. The present parameterization tends to give spectra that are still too narrow at high frequencies (figure 3), but generally too broad.

For all these issues, we are seeking a general improvement of the physical basis of the source functions. In particular, work on the wave breaking term should eventually separate the term in a breaking probability, expressed as a properly weighted convolution integral over the spectrum, and a breaking severity [35]. Because individual waves break, one has to go from the spectrum to the individual waves, for which breaking statistics can be verified, and back to the spectrum. The source term should thus be a deconvolution of this dissipation per breaking scale, back to the Fourier modes that contribute to a given scale, as proposed by [22]. With that approach, the use of both B and B_0 as measures of the saturation level may not be necessary and B may suffice. Redefining B based on general wave kinematics (deep and shallow water) may provide a generic wave breaking term for both deep and shallow water, avoiding the arbitrary but usual decomposition in white-capping and depth-induced breaking. Based on the altimeter mss_C data, the wave kinematics contained in B and the threshold B_r should also include the straining of short waves by long waves, which likely enhance their breaking probabilities and severities, an effect consistent with the reduction of observed mean square slopes with the presence of swell [17]. These observations also support the reduction of wind input for the shorter waves caused by a swell-induced reduction of atmospheric turbulence [36].

The convolution-deconvolution approach, in both the directional and frequency domains, still has to be implemented and calibrated. Estimating reliable breaking statistics will be useful for reproducing the enhanced generation of breaking waves [37] in the wind generation term, and for the parameterization of the cumulative breaking effect [9], as well as for many remote sensing and offshore engineering applications.

ACKNOWLEDGMENT

This research was made possible by the support of ECMWF and Meteo-France, providing wind and ice fields, ESA and CNES providing satellite altimeter data, and all contributors to the JCOMM (WMO-IOC) exchange program, including NOAA/NDBC, Meteo-France, Puertos del Estado, the U.K. Met. Office, the Australian Weather Bureau and the Irish Marine Institute for the many in situ observations. The quality of the model and feasibility of our research owes much to the very kind help by H. L. Tolman (NOAA/NCEP), J. Bidlot and P. Janssen (ECMWF). Y. Quilfen and D. Croizé-Fillon (Ifremer) helped with the JASON σ_0 data, and performed the comparison of model and altimeter H_s data. This work was partially funded by the ANR project HEXECO.

REFERENCES

[1] Gelci, R., Cazalé, H., Vassal, J., 1957. Prévision de la houle. La méthode des densités spectroangulaires. Bulletin d'information du Comité d'Océanographie et d'Etude des Côtes 9, 416–435.

[2] Hasselmann, K., 1962. On the non-linear energy transfer in a gravity wave spectrum, part 1: general theory. J. Fluid Mech. 12, 481–501.

[3] Janssen, P. A., Onorato, M., 2005. The shallow water limit of the zakharov equation and consequences for (freak) wave prediction. Tech. Rep. Memomrandum 464, Research Department, ECMWF, Reading, U. K.

[4] WISE Group, 2007. Wave modelling the state of the art. Progress in Oceanography, 75, 603–674.

[5] Ardhuin, F., O'Reilly, W. C., Herbers, T. H. C., Jessen, P. F., 2003. Swell transformation across the continental shelf. part I: Attenuation and directional broadening. J. Phys. Oceanogr., 33, 1921–1939.

[6] Elgar, S., Raubenheimer, B., 2008. Wave dissipation by muddy seafloors. Geophys. Res. Lett., 35, L07611.

[7] Cavaleri, L., 2006. Wave modeling where to go in the future. Bull. Amer. Meterol. Soc., 87 (2), 207–214.

[8] Banner, M. L., Babanin, A. V., Young, I. R., 2000. Breaking probability for dominant waves on the sea surface. J. Phys. Oceanogr., 30, 3145–3160.

[9] Babanin, A. V., Young, I. R., 2005. Two-phase behaviour of the spectral dissipation of wind waves. In: Proceedings of the 5th International Symposium Ocean Wave Measurement and Analysis, Madrid, june 2005. ASCE, paper number 51.

[10] Ardhuin, F., Chapron, B., Collard, F., 2008. Ocean swell evolution from distant storms. Unpublished manuscript.

[11] Komen, G. J., Hasselmann, K., Hasselmann, S., 1984. On the existence of a fully developed windsea spectrum. J. Phys. Oceanogr., 14, 1271–1285.

[12] Bidlot, J., Abdalla, S., Janssen, P., 2005. A revised formulation for ocean wave dissipation in CY25R1. Tech. Rep. Memorandum R60.9/JB/0516, Research Department, ECMWF, Reading, U. K.

[13] Alves, J. H. G. M., Banner, M. L., 2003. Performance of a saturation-based dissipation-rate source term in modeling the fetch-limited evolution of wind waves. J. Phys. Oceanogr., 33, 1274–1298.

[14] Ardhuin, F., Herbers, T. H. C., Watts, K. P., van Vledder, G. P., Jensen, R., Graber, H., 2007. Swell and slanting fetch effects on wind wave growth. J. Phys. Oceanogr. 37 (4), 908–931.

[15] Hauser, D., Caudal, G., Guimbard, S., and Mouche, A. A., 2008, A study of the slope probability density function of the ocean waves from radar observations, J. Geophys. Res., 113, C02006, C02006.

[16] Barrick, D. E., 1968, Rough surface scattering based on the specular point theory," IEEE Trans. Antennas Propagat., vol. AP-14, 449-454.

[17] Vandemark, D., Chapron, B., Sun, J., Crescenti, G. H., and Graber, H. C. , 2004, Ocean wave slope observations using radar backscatter and laser altimeters, J. Phys. Oceanogr., 34, 2825-2842.

[18] Tolman, H. L., Chalikov, D., 1996. Source terms in a third-generation wind wave model. J. Phys. Oceanogr., 26, 2497–2518.

[19] Banner, M. L., Gemmrich, J. R., Farmer, D. M., 2002. Multiscale measurement of ocean wave breaking probability. J. Phys. Oceanogr., 32, 3364–3374.

[20] Stansell, P., MacFarlane C., 2002, Experimental investigation of wave breaking criteria based on wave phase speeds. J. Phys. Oceanogr., 32, 1269-1283.

[21] Wu, C. H., Nepf, H. M., 2002, Breaking criteria and energy losses for three-dimensional wave breaking, J. Geophys. Res., 107(C10), 3177.

[22] Papadimitrakis, Y. A., 2006, On the probability of wave breaking in deep waters, Deep Sea Res. II, 52, 1246-1269.

[23] J.-F. Filipot, F. Ardhuin, and A. Babanin, 2008, Paramétrage du déferlement des vagues dans les modèles spectraux : approches

semi-empirique et physique, in Actes des Xèmes journées Génie côtier-Génie civil, Sophia Antipolis, Centre Français du Littoral.

[24] Tolman, H. L., 2007. The 2007 release of WAVEWATCH III. In: Proceedings, 10th Int.Workshop of Wave Hindcasting and Forecasting, Hawaii.

[25] Hasselmann, S., Hasselmann, K., Allender, J., and Barnett, T., 1985, Computation and parameterizations of the nonlinear energy transfer in a gravity-wave spectrum. Part II: Parameterizations of the nonlinear energy transfer for application in wave models, J. Phys. Oceanogr., 15, 1378-1391.

[26] Ardhuin, F., Jenkins, A. D., 2006. On the interaction of surface waves and upper ocean turbulence. J. Phys. Oceanogr. 36 (3), 551–557.

[27] Kudryavtsev, V. N., Makin, V. K., 2004. Impact of swell on the marine atmospheric boundary layer. J. Phys. Oceanogr. 34, 934–949.

[28] Harris, D. L., 1966. The wave-driven wind. J. Atmos. Sci. 23, 688–693.

[29] Dore, B. D., 1978. Some effects of the air-water interface on gravity waves. Geophys. Astrophys. Fluid. Dyn. 10, 215–230.

[30] Jensen, B. L., Sumer, B. M., Fredsøe, J., 1989. Turbulent oscillatory boundary layers at high Reynolds numbers. J. Fluid Mech., 206, 265–297.

[31] Grant,W. D., Madsen, O. S., 1979. Combined wave and current interaction with a rough bottom. J. Geophys. Res., 84, 1797–1808.

[32] Tolman, H. L., 2003.Treatment of unresolved islands and ice in wind wave models. Ocean Modelling, 5, 219–231.

[33] Rascle, N., Ardhuin, F., Queffeulou, P., Croizé-Fillon, D., 2008. A global wave parameter database for wave-current-turbulence interaction studies. Ocean Modelling (accepted for publication).

[34] Cavaleri, L., Missing the peaks, oral presentation at the 2008 WISE Meeting, Helsinki, Finland.

[35] Manasseh, R., Babanin, A. V., Forbes, C., Rickards, K., Bobevski, I., and Ooi, A., Passive acoustic determination of wave-breaking events and their severity across the spectrum, J. Atmos. Ocean Technol., vol. 23, pp. 599-618, 2006.

[36] Sullivan, P. P., Edson, J. B., Hristov, T., & McWilliams, J. C., 2008, Large-Eddy Simulations and observations of atmospheric marine boundary layers above non-equilibrium surface waves, J. Atmos. Sci., 65,1225–1244.

[37] N. Reul, H. Branger, and J.-P. Giovanangeli, Air flow structure over short-gravity breaking water waves, Boundary-Layer Meteorol., vol. 126, 2008